

Analysis of Sea Surface Temperature and Containing Water Chlorophyll-A Distribution Using Gee (Google Earth Engine) Code Technology in Sibolga Waters

Mardame Pangihutan Sinaga^{1,*}, Jono Barita Sianipar², Ady Frenly Simanullang³,
Herna Febrianty Sianipar⁴, Ewin Handoco S⁵, Goldberd Harmuda Duva Sinaga⁶

^{1,3,4,5} University of HKBP Nommensen Pematangsiantar / Water Resource Management / Research / Sangnawaluh Street #4, Siopat Suhu Village, Siantar Timur District. Province of North Sumatra. Area Code: 21139. ² Lab Data Spatial.

⁶ Universitas HKBP Nommensen Medan. Province of North Sumatra.

Corresponding Author e-mail: m.pangihutan@gmail.com

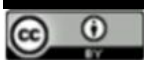
Received: October 18, 2022

Accepted: March 06, 2023

Published: March 06, 2023

Copyright © 2023 by author(s) and
Scientific Research Publishing Inc.

Open Access



Abstract

Research on SST and containing water chlorophyll-a using GEE Cloud technology in Sibolga Waters has been carried out since February-December 2019. The analysis was carried out using the MODIS AQUA-L3SMI satellite. The SST results showed that it spread evenly from the coast of Sibolga to the sea, which was 28-33 °C and did not fluctuate, while the containing water of chlorophyll-a spread evenly, from February-April with a value of 0,1-1 mg/m³ varied, namely from June-August, and fluctuations namely in October-December 2019 with an amount of 0,5-2 mg/m³. SST spreads evenly, varies, and fluctuates around the outskirts of Sibolga coastal waters to the middle of Sibolga Waters, which is unsuitable for demersal fish species. Meanwhile, the containing water chlorophyll-a spreads evenly watered and fluctuates. The high containing water chlorophyll-a in all waters and the high SST will make a certain type of fish that can live, namely carnivorous fish species. Image data can be used to map SST distribution patterns and containing water chlorophyll-a in Sibolga Waters.

Keywords: Sea Surface Temperature (SST), Chlorophyll-a, MODIS AQUA-L3SMI satellite, Sibolga Waters.

1. Introduction

Sub Introduction

Sibolga waters are strategically located as a center for marine fishery production in North Sumatra. The catch produced by the fisherman of Sibolga consists of pelagic and demersal fish. The large potential for fishing in Sibolga Waters has not been utilized optimally because in determining fishing areas, fishermen still use intuition or instincts that have been passed down from generation to generation. This is not in line with technological advances because the use of instincts is sometimes inaccurate and untested. Therefore, there is a need for research and development of fishing systems using remote sensing technology based on oceanographic conditions.

Remote sensing technology is one of the sources of information in collecting marine data effectively and efficiently, and remote sensing covers a wide area of study, the accuracy is relatively high, and the process requires less time and costs which is shorter than field surveys. Several products from satellite

imagery provide Information about a water image, including several types of satellite imagery, namely Landsat, SPOT, Quick Bird, Worldview-2, and Modis Aqua images. The satellite image used to determine the distribution of Sea Surface Temperature (SST) containing water chlorophyll-a in Belawan Waters is Modis Aqua with a spatial resolution of 10 meters.

Satellite imagery is the result of remote sensing observations. One of the MODIS image products is SST and chlorophyll-a estimation, and chlorophyll-a values can be obtained by direct measurement or by remote sensing satellite data extraction. The use of remote sensing data will be faster, more effective, and more efficient and can cover a wider coverage area when compared to direct measurement which requires more costs and energy, while the coverage area is relatively small. SST and chlorophyll-a are oceanographic factors that are quite important for the life of organisms in the waters.

Temperature and chlorophyll-a are oceanographic parameters that affect fish distribution (demersal) and water fertility. Demersal fish will be

distributed in warm waters and contain lots of phytoplankton because demersal fish eat small fish. Therefore, it is necessary to analyze the relationship between the distribution pattern of tuna with SST and chlorophyll-a to estimate the distribution area of demersal fish using remote sensing by considering water parameters associated with the behavior and preferences of demersal fish. The fishing ground can save time and money and get maximum catch.

The purpose of this research was to analyze the distribution of Sea Surface Temperature (SST) and containing water chlorophyll-a using MODIS AQUA-L3SMI in Sibolga and surrounding waters before and after rainfall, expanding rainfall to SST and chlorophyll-a containing water to wide waters around Sibolga Waters, and it is necessary to study rainfall discharge on SST and chlorophyll-a containing water, which is basic information for other researches in further research to determine the effect of SST and chlorophyll-a containing water in living tissue, as a reference source in management Sibolga Water is more environmentally friendly and as information for the local government and also residents living in the waters of Sibolga.

2. Methodology

This research was carried out in January-December 2019. This period includes data collection, data analysis, and processing, as well as the preparation of the final report. The location for data collection is around Sibolga Waters, North Sumatera Province. As shown in the location map in Figure 1, data processing and analysis were carried out at the GIS Laboratory of study program water resources management.



Fig 1. Map of Research Location.

Methods and Tools

Data

The data source of MODIS AQUA-L3SMI satellite imagery obtained from NASA is downloaded through the website: <https://earthengine.google.com/>.

Equipment

The tools and materials used in this study are tabulated in Table 1.

Table 1. Tools and Materials used during data processing.

Materials	Function
Data in situ TSS	Secondary Data (9 stations)
Citra Satelit Sentinel-2	Primary Data
Rainfall	Secondary Data
Data Analysis Tool	Function

Laptop	Data Analysis
Ms. Excel 2016	Data processing and calculation
ArcGis 10.5	Map Visualization

Methods

MODIS AQUA-L3SMI image processing in the analysis of SST and containing water chlorophyll-a using GEE Cloud is divided into several processes, namely searching for Indonesia in **Search Places and Datasets**, taking **Collection Snippets**, resampling (geometric correction), masking (separating land and sea), reclassify and visualize in map form.

1. Search Indonesia on Search Places and Datasets.

Make ROI in the form of a box (draw a rectangle) above the state of Indonesia, and change 'geometry' become 'roi'.

2. Taking Collection Snippet

Collection Snippet retrieval in an early stage in image processing. The collection snippet process starts with importing or copying "ee.ImageCollection('NASA/OCEANDATA/MODIS-Aqua/L3SMI') into the script in <https://code.earthengine.google.com/>.

3. Filtering

The filtering of the data to be obtained is carried out using the observation date period. The observations' start date and end date to be studied must be entered to obtain data.

```

4 var remoteSensingReflectance =
5   dataset.select(['sst']).median();
6 var remoteSensingReflectanceVis = {
7   min: -2,
8   max: 40,
9   palette: ['040274', '040281', '0502a3', '0502b8', '0502ce', '0502e6',
10  '0602ff', '235c01', '307ef3', '269db1', '30c8e2', '32d3ef',
11  '3be25f', '3ff38f', '86e26f', '3ae237', 'b5e22e', 'd6e21f',
12  'fff705', 'ffd611', 'ffb613', 'ffb813', 'ffe008', 'ffa00d',
13  'ff0000', 'de0001', 'c21301', 'a71001', '911003']
14 };
15
16 Map.centerObject(roi, 4);
17 Map.addLayer(
18   remoteSensingReflectance, remoteSensingReflectanceVis,
19   'MODIS SST 2019');

```

Retrieval of the selected data and the mean of the set.

```

spi sibolga 2019_2
Get Link Save Run Reset Apps
Imports (1 entry)
var roi: Polygon, 4 vertices
1 var dataset = ee.ImageCollection('NASA/OCEANDATA/MODIS-Aqua/L3SMI')
2   .filterDate('2019-01-01', '2019-12-31')
3   .map(function(dataset){return dataset.clip(roi)});

```

Image collection and the results of the retrieval are stored in the variable dataset.

Fig 2. Filtering the data

4. Taking SST and chlorophyll-a Value

Taking the 'sst' and 'chlorophyll-a' band value from each image set in the dataset variable, and then taking the median value to be the SST and chlorophyll-a value stored in the *remoteSensingReflectance* variable. The 'sst' and 'chlorophyll-a' band value is already reflectance value.

5. Displays a map of SST and chlorophyll-a

The results of taking the SST and chlorophyll-a value are then displayed on the monitor by setting the

visualization parameters
 "remoteSensingReflectanceVis".

6. Esport Map to Google Drive

Transferring the resulting data in the map form by exporting the map to Google Drive. Then, the exported map (*.tiff) is transferred to ArcGIS to view the resulting SST and chlorophyll-a data.

```

spl sibolga 2019_2
Get Link Save Run Reset Apps
Imports (1 entry)
var roi: Polygon, 4 vertices
1 var dataset = ee.ImageCollection("NASA/OCEANDATA/MODIS-Aqua/L3SMI")
2   .filterDate('2019-01-01', '2019-12-31')
3   .map(function(dataset){return dataset.clip(roi)});
4 var remoteSensingReflectance =
5   dataset.select(['sst']).median();
6 var remoteSensingReflectanceVis = {
7   min: -2,
8   max: 40,
9   palette: ['040274', '040281', '0502a3', '0502b8', '0502ce', '0502e6',
10  '0602ff', '235cb1', '307ef3', '269db1', '30c8e2', '32d3ef',
11  '3be285', '3ff38f', '86e26f', '3ae237', 'b5e22e', 'd6e21f',
12  'fff705', 'ffe611', 'ffb613', 'ffa813', 'ffa608', 'ffa60d',
13  'ffa608', 'de0001', 'c21301', 'a71801', '911803'];
14 };
15
16 Map.centerObject(roi, 4);
17 Map.addLayer(
18   remoteSensingReflectance, remoteSensingReflectanceVis,
19   'MODIS SST 2019');
20
21 var palette = ['blue', 'yellow', 'red', 'brown']
22
23 //print(maxSST)
24
25 var vizSST = {
26   min: 20,
27   max: 40,
28   palette: palette
29 }
30
31 function createColorBar(titleText, palette, min, max) {
32   // Legend title
33   var title = ui.Label({
34     value: titleText,
35     style: {fontWeight: 'bold', textAlign: 'center', stretch: 'horizontal'}});
36
37   // Colorbar
38   var legend = ui.Thumbnail({
39     image: ee.Image.pixelonLat().select(0),
40     params: {
41       bbox: [0, 0, 1, 0.1],
42       dimensions: '200x20',
43       format: 'png',
44       min: 0, max: 1,
45       palette: palette},
46     });
47
48   // Create a panel with all widgets
49   var legendPanel = ui.Panel({
50     widgets: [title, legend, ui.Label({
51       value: 'SST',
52       style: {fontWeight: 'bold', stretch: 'horizontal'}}),
53     ui.Label({value: 'min: ' + min, stretch: 'horizontal'}),
54     ui.Label({value: 'max: ' + max, stretch: 'horizontal'})],
55     layout: ui.Panel.Layout.Flow('horizontal')});
56
57 // Create a panel with all widgets
58 var legendPanel = ui.Panel({
59   widgets: [title, legend, ui.Label({
60     value: 'SST',
61     style: {fontWeight: 'bold', stretch: 'horizontal'}}),
62     ui.Label({value: 'min: ' + min, stretch: 'horizontal'}),
63     ui.Label({value: 'max: ' + max, stretch: 'horizontal'})],
64     layout: ui.Panel.Layout.Flow('horizontal')});
65
66 // Call the function to create a colorbar legend
67 var colorBar = createColorBar('Sea Surface Temperature / SST', 'celsius', min, max);
68
69 // Create a panel
70 var legendPanel = ui.Panel({
71   widgets: [colorBar, ui.Label({value: 'min: ' + min, stretch: 'horizontal'}),
72     ui.Label({value: 'max: ' + max, stretch: 'horizontal'})],
73     layout: ui.Panel.Layout.Flow('horizontal')});
74
75 // Add the legend panel to the map
76 Map.addLayer(legendPanel, {min: 0, max: 40, palette: palette});
77
78 // Add the legend panel to the map
79 Map.addLayer(legendPanel, {min: 0, max: 40, palette: palette});
80
81 // Add the legend panel to the map
82 Map.addLayer(legendPanel, {min: 0, max: 40, palette: palette});
83
84 // Add the legend panel to the map
85 Map.addLayer(legendPanel, {min: 0, max: 40, palette: palette});
86
87 // Add the legend panel to the map
88 Map.addLayer(legendPanel, {min: 0, max: 40, palette: palette});
89
90 // Add the legend panel to the map
91 Map.addLayer(legendPanel, {min: 0, max: 40, palette: palette});
92
93 // Add the legend panel to the map
94 Map.addLayer(legendPanel, {min: 0, max: 40, palette: palette});
95
96 // Add the legend panel to the map
97 Map.addLayer(legendPanel, {min: 0, max: 40, palette: palette});
98
99 // Add the legend panel to the map
100 Map.addLayer(legendPanel, {min: 0, max: 40, palette: palette});
101
102 // Add the legend panel to the map
103 Map.addLayer(legendPanel, {min: 0, max: 40, palette: palette});
104
105 // Add the legend panel to the map
106 Map.addLayer(legendPanel, {min: 0, max: 40, palette: palette});
107
108 // Add the legend panel to the map
109 Map.addLayer(legendPanel, {min: 0, max: 40, palette: palette});
110
111 // Add the legend panel to the map
112 Map.addLayer(legendPanel, {min: 0, max: 40, palette: palette});
113
114 // Add the legend panel to the map
115 Map.addLayer(legendPanel, {min: 0, max: 40, palette: palette});
116
117 // Add the legend panel to the map
118 Map.addLayer(legendPanel, {min: 0, max: 40, palette: palette});
119
120 // Add the legend panel to the map
121 Map.addLayer(legendPanel, {min: 0, max: 40, palette: palette});
122
123 // Add the legend panel to the map
124 Map.addLayer(legendPanel, {min: 0, max: 40, palette: palette});
125
126 // Add the legend panel to the map
127 Map.addLayer(legendPanel, {min: 0, max: 40, palette: palette});
128
129 // Add the legend panel to the map
130 Map.addLayer(legendPanel, {min: 0, max: 40, palette: palette});
131
132 // Add the legend panel to the map
133 Map.addLayer(legendPanel, {min: 0, max: 40, palette: palette});
134
135 // Add the legend panel to the map
136 Map.addLayer(legendPanel, {min: 0, max: 40, palette: palette});
137
138 // Add the legend panel to the map
139 Map.addLayer(legendPanel, {min: 0, max: 40, palette: palette});
140
141 // Add the legend panel to the map
142 Map.addLayer(legendPanel, {min: 0, max: 40, palette: palette});
143
144 // Add the legend panel to the map
145 Map.addLayer(legendPanel, {min: 0, max: 40, palette: palette});
146
147 // Add the legend panel to the map
148 Map.addLayer(legendPanel, {min: 0, max: 40, palette: palette});
149
150 // Add the legend panel to the map
151 Map.addLayer(legendPanel, {min: 0, max: 40, palette: palette});
152
153 // Add the legend panel to the map
154 Map.addLayer(legendPanel, {min: 0, max: 40, palette: palette});
155
156 // Add the legend panel to the map
157 Map.addLayer(legendPanel, {min: 0, max: 40, palette: palette});
158
159 // Add the legend panel to the map
160 Map.addLayer(legendPanel, {min: 0, max: 40, palette: palette});
161
162 // Add the legend panel to the map
163 Map.addLayer(legendPanel, {min: 0, max: 40, palette: palette});
164
165 // Add the legend panel to the map
166 Map.addLayer(legendPanel, {min: 0, max: 40, palette: palette});
167
168 // Add the legend panel to the map
169 Map.addLayer(legendPanel, {min: 0, max: 40, palette: palette});
169
    
```

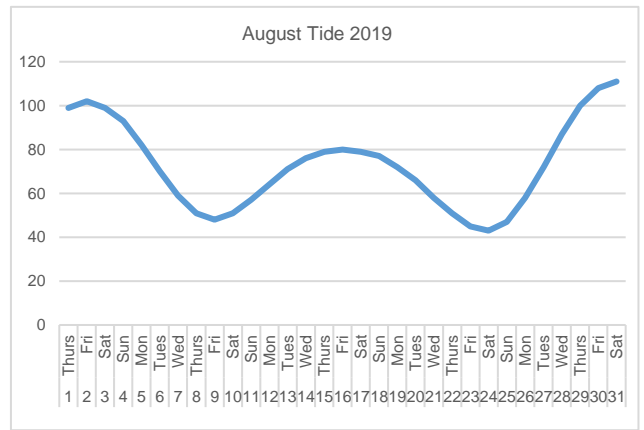
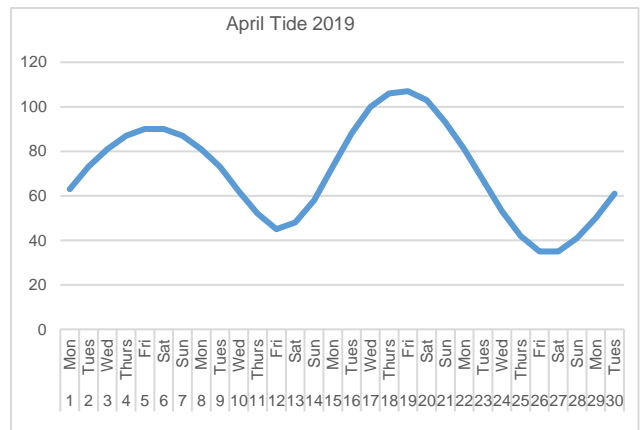
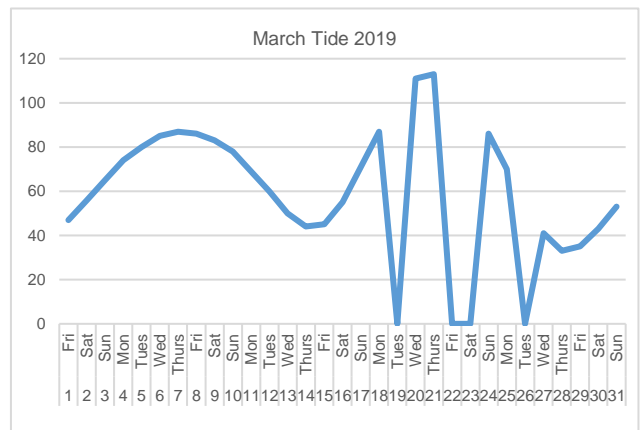
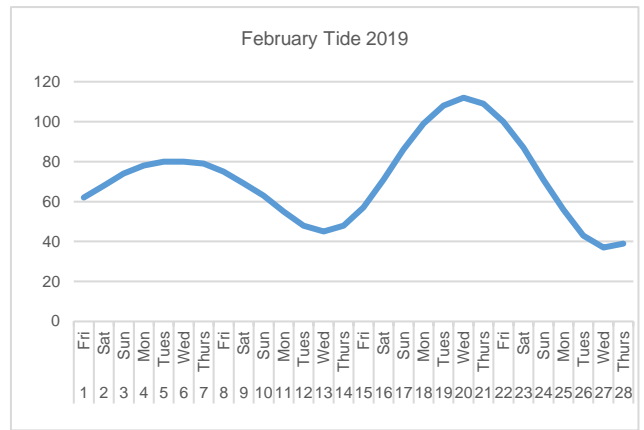
Fig 3. Transferring the resulting data

Results and Discussion

1. Results

Tide

The tidal phenomenon is a process that occurs in the sea continuously. This natural process occurs due to the gravitational force of the sun, moon, and celestial bodies that attract each other so that the parts of the earth that are close to the celestial bodies will experience tides, while in other parts of the earth, there will be receding.



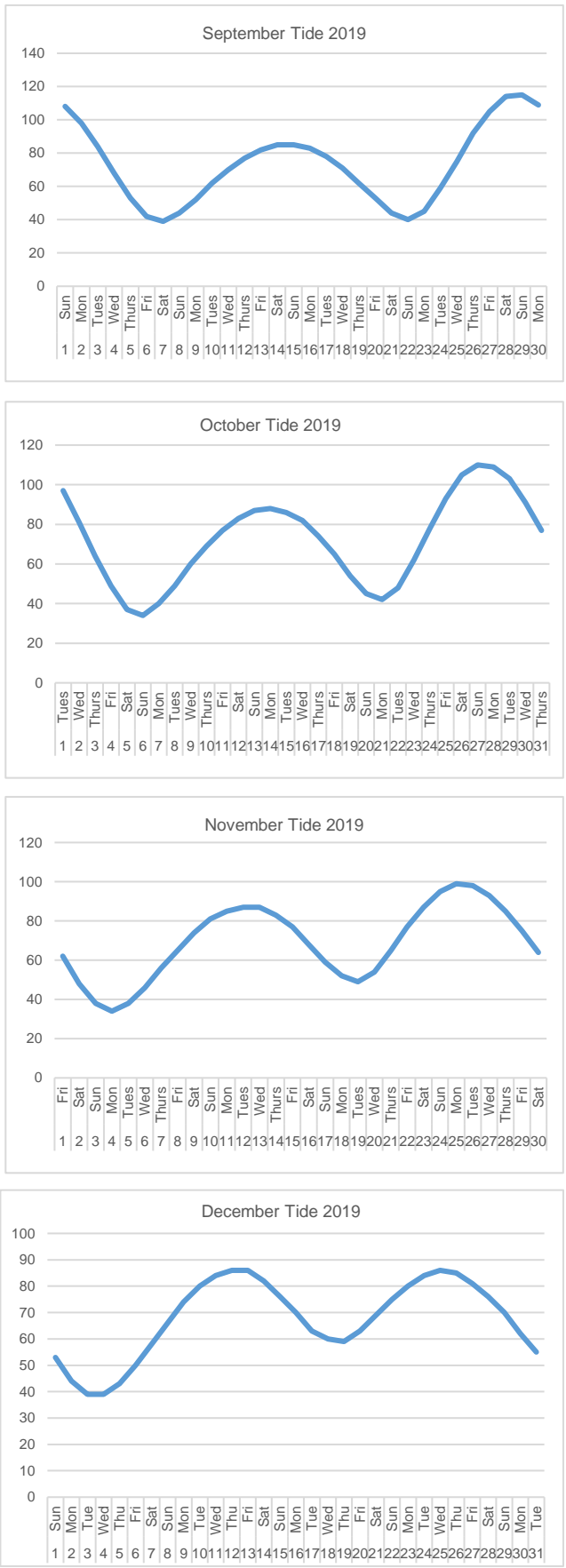


Fig 4. Real-time prediction tides in February-December 2019.

Rainfall

Precipitation is water released from clouds as rain, snow, or hail. Precipitation begins after water vapor condensed in the atmosphere becomes too heavy to remain in the atmospheric air currents and falls.

The stages of the rain process:

- 1. Evaporation**
Evaporation is changing liquid water into gaseous water (evaporation). This allows the gas to rise above the Earth's atmosphere. The higher the sun's heat, the more amount of water becomes water vapor and rises to the earth's atmosphere.
- 2. Transpiration**
The other stage is the evaporation of water. Evaporation of water does not only occur in the soil but also takes place in the tissues of living things. The working principle of transpiration with evaporation is almost the same. Both turn water into water vapor which rises to the top of the atmosphere.
- 3. Condensation.**
Transpiration is the process of evaporation in plants when they breathe. However, the amount of water that becomes vapor through transpiration is generally much less than the amount of water vapor produced by evaporation.

Furthermore, water vapor undergoes condensation or condensation in the form of ice particles. Changes in form occur due to the influence of very low air temperature at that altitude.

The ice particles are then formed into saturated clouds which will then be the beginning of the process of rain.

- 4. Precipitation (Rain)**
This stage is the stage of the occurrence of rain. The reason is that the saturated clouds containing water droplets in the atmosphere get colder at this stage. This makes the clouds heavier until finally the water droplets they contain fall to the earth's surface.

The fall of water droplets from the atmosphere to the earth's surface is called rain. If the ambient temperature is less than 0 °C, snow or ice is likely to occur.

Rainwater has fallen to the ground, some will seep into the ground as groundwater—some flows into lakes or rivers which then flow into the sea.

The phenomenon of rainfall that occurred in Sibolga Waters for 5 months can be seen in Figures 5-8. This natural process occurs due to too much water vapor being stored so that the clouds cannot accommodate the water vapor and fall to the earth.

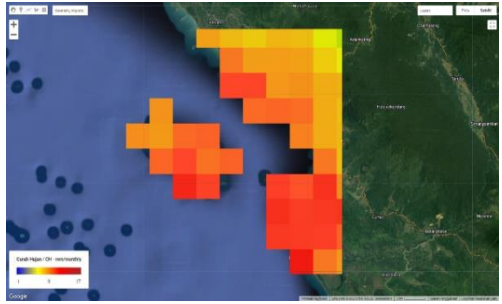


Fig 5. Sibolga City Rainfall from Feb 1st - 31st March 2019.

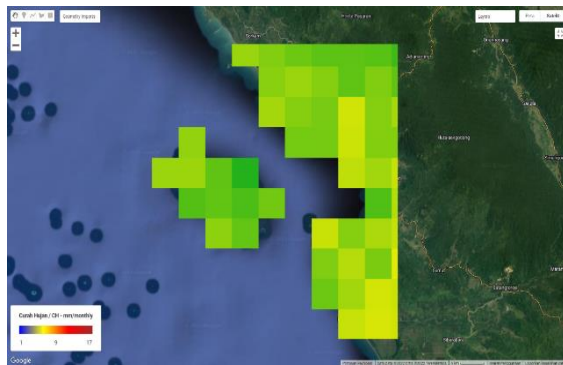


Fig 6. Sibolga City Rainfall from March 1st - 30th, April 2019.



Fig 7. Sibolga City Rainfall from June 1st - 31st, August 2019.

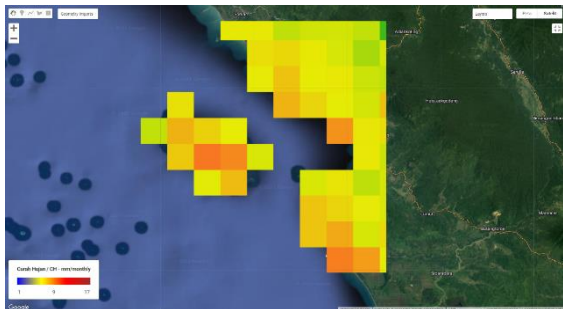


Fig 8. Sibolga City Rainfall from Oct 1st - Dec 31st, 2019.

Analysis of the SST Distribution and Chlorophyll-a using GEE Cloud.

The Modis Aqua-L3SMI image analysis does not require radiometric correction because the value of the image is already a reflectance value. Geometric analysis is also not needed because this study only focuses on the reflectance value of the image. The image used is the Modis Aqua-L3SMI image with the recording date at high tide and rainfall in 2019.

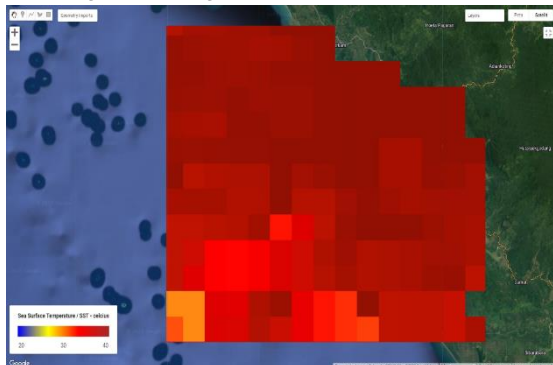


Fig 9. SST Analysis from Feb 1st - March 31st, 2019.

Map of the SST distribution on February 1st - March 31st 2019 (Figure 9) and image recording show that at high tide and high rainy season, the highest SST value is 31,98-32,94 °C, and the lowest SST value is 29,77-30,87 °C. the highest and lowest SST values spread to all the outskirts of Sibolga Waters and all river waters leading to Sibolga Waters, namely red and orange.



Fig 10. SST Analysis from March 1st - April 30th, 2019.

SST distribution map on March 1st – April 30th, 2019 (Figure 10) and image recording show that at high tide positions and during the high rainy season, the SST value is 31,95-32,985 °C and the lowest SST value is 29,9-30,995 °C. This happens for all Sibolga Waters.

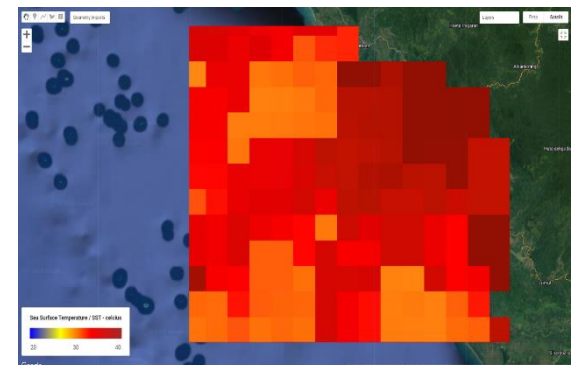


Fig 11. SST Analysis from June 1st - August 30th, 2019.

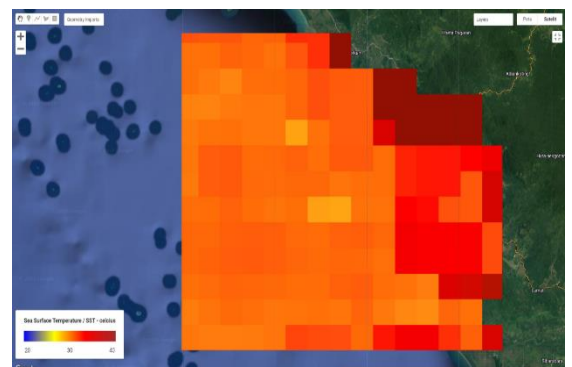


Fig 12. SST Analysis from Oct 1st - Dec 31st, 2019.

In October-December 2019, the temperature of water in the coastal areas was higher than the waters farther from the coast. It is suspected that because of the rain, the intensity of the sunlight is low and tends to be a lot towards the coast. Coastal areas will heat up quickly after the rainy season and in contrast to waters farther from the coast.

The distribution of SST for the months of February-March 2019 varies, cold water masses do not reach the coast of Sibolga Waters and hot water masses occur throughout Sibolga Waters. Similar to the distribution of SST for March-April 2019, which is more varied, cold water masses tend to be absent from the coast to the coast of Sibolga and Murshala Waters. The mass of hot water tends to be evenly distributed to all waters and coastal areas of Sibolga.

The SST distribution for the months of June-August 2019 varies, the hot water mass is also absent, and tends to partly spread to the north and south of Sibolga Waters and evenly to the Sibolga coastal area.

In February-March 2019, March-April 2019, June-October 2019, and October-December 2019 there was a very high intensity of solar radiation on the calm sea surface which caused higher heat absorption into seawater so that the water temperature rose. In the opinion of Sverdrup *et al.*, (1942), processes such as the absorption of radiation from the sun, the flow of heat from the earth through the seabed, changes in the form of kinetic energy into heat energy, the heat flow from the atmosphere through the air to the sea and condensation of water vapor accompanied by the release of heat occurs in the sea will increase the temperature of seawater. Furthermore, the processes of back radiation from the sea surface, heat flow (convection) to the atmosphere, and evaporation can reduce the temperature of seawater in the surface layers of the waters.

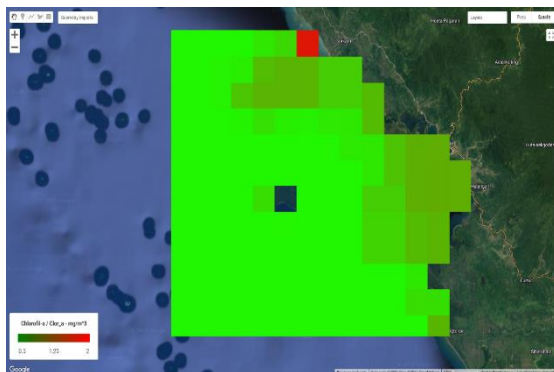


Fig 13. Chlorophyll-a Analysis from Feb 1st - March 31st, 2019.

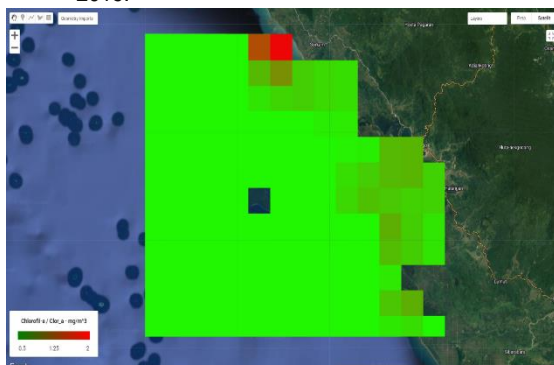


Fig 14. Chlorophyll-a Analysis from March 1st - April 30th, 2019.

The concentration of chlorophyll-a in February 1st - March 31st 2019 was concentrated in the Murshala Waters due to a large number of coral reef areas around the Murshala coastal waters, while the Sibolga coastal area had a small amount of

chlorophyll-a. For Sorkam Waters where there is no chlorophyll-a. Coral reefs can hold plankton carried by currents from the open waters to the coastal waters of Sibolga. According to LIPI (2007), the waters of Sibolga have a lot of coral reefs, amounting to 4.422.829 ha, and mangroves have an area of 1.823.436 ha which are located in the mainland area of Sibolga, Murshala Island and its surroundings, causing fishing trawlers to catch fish around the Sibolga Waters.

Furthermore, Parson *et al.*, (1984) suggested that it is not easy to explain generally accepted conditions regarding the horizontal distribution of phytoplankton in the sea. Caused by differences in ecological conditions in different parts of the sea, such as in coastal and estuary areas, and coastal and high seas. There is a tendency for the distribution of phytoplankton to be more clustered in the oceanic (offshore) area.

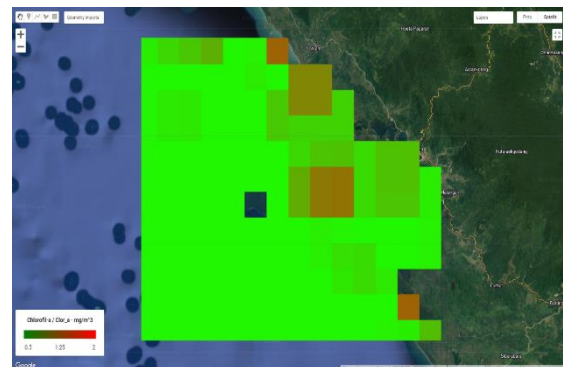


Fig 15. Chlorophyll-a Analysis from June 1st - August 30th, 2019.

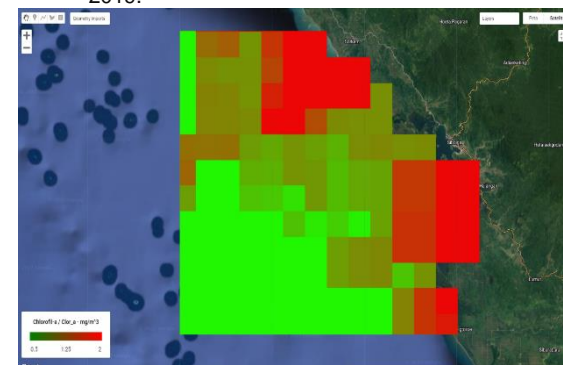


Fig 16. Chlorophyll-a Analysis from October 1st - December 30th, 2019.

The spatial distribution of chlorophyll-a concentration for March 1st - April 30th, 2019 (Figure 14), tends to move from the coastal waters of Sorkam to the sea waters of Sibolga and slightly in the coastal areas of Sibolga, as well as the amount of chlorophyll-a for June 1st - August 30th, 2019 (Figure 15), the distribution of chlorophyll-a concentrations moving widely from the mainland to the waters of Murshala, slightly in the waters of Sibolga leading to the waters of the Sibolga sea.

Meanwhile, the chlorophyll-a concentration distribution in October-December 2019, spread from the Murshala coastal waters to the Sibolga sea. The concentration of chlorophyll-a in the coastal areas of Sibolga and Sorkam was absent and slightly towards the Sibolga Waters (Figure 16).

The high chlorophyll-a in Sibolga coastal waters for February-March 2019, March-April 2019, and

June-August 2019 compared to October-December 2019, is most likely due to physical and chemical factors. In the opinion of Arinardi *et al.*, (1997), plankton in the sea, in general, are not spread evenly but live in groups. As a result of physical and chemical processes in coastal waters, groups of plankton are more common in neritic waters (especially estuary-influenced waters) than in oceanic waters. The productivity of coastal waters is determined by several factors such as tidal currents, morphogeography, and physical processes from offshore. In addition, Sujoko *et al.*, (2002) in Sinaga (2009) said that sea surface currents can carry phytoplankton and other nutrients following the speed and pattern of a current movement or caused by currents themselves with another current in the vicinity. It can be determined that the density of phytoplankton is influenced by sea surface currents.

The low chlorophyll-a in October-December 2019 was suspected of physical and biological influences. In the opinion of Arinardi *et al.*, (1997), the causes of grouping are broadly distinguished by physical and biological influences. Physical effects can be caused by turbulence or advection (the movement of large water masses containing plankton in it). Wind can also cause the accumulation of plankton in certain places such as along the coast under the current (leeward side). Biological influence occurs when there are differences in the growth of phytoplankton and the speed of diffusion to move away from the group and the presence of predators from phytoplankton.

The concentration of chlorophyll-a in the oceans has different values vertically because it is influenced by oceanographic factors such as SST, wind, currents, and others. Fluctuations in these values can be observed by measuring directly or by using sensing technology. The concentration of chlorophyll-a in water can give a distinctive sea hue so that through the sensing methods using satellite vehicles, the pigment concentration can be estimated.

The temporal distribution of chlorophyll-a containing water in Sibolga Waters generally varies. This is the opinion of Parson *et al.*, (1984) who state that the vertical distribution of chlorophyll-a in the ocean generally differs with time, and sometimes it is found to be maximum near the surface, but at other times it may be more concentrated at the bottom of the euphotic depth. According to the opinion of Setiapermana *et al.*, (1992) the fact obtained from their research is that the eastern Indian Ocean and Arinardi (1995) in Jakarta Bay showed differences in the distribution of chlorophyll-a in different seasons.

Furthermore, Gabric and Parslow (1989) suggested that the rate of primary productivity in the aquatic environment is determined by physical factors. The main physical factors controlling phytoplankton production in eutrophic waters are vertical mixing, light penetration in the water column, and the sinking rate of phytoplankton cells. The vertical mixing of water masses plays a very important role in fertilizing the water column, namely by lifting nutrients from the deep layers to the surface layers. With the increase in nutrients in the surface layer and assisted by sufficient sunlight penetration in the water column, it can increase the rate of

primary productivity through the photosynthetic activity of phytoplankton.

Phytoplankton as plants containing the pigment chlorophyll-a can carry out photosynthetic reactions where water and carbon dioxide in the presence of sunlight and nutrient salts can produce organic compounds such as carbohydrates. Because of the ability to form organic substances from inorganic substances, phytoplankton is referred to as primary producers. In Figure 5-8, it can be seen that the value of in-situ SST data using GEE Cloud is not the same. This may be due to the time of in situ data acquisition being influenced by clouds or high rainfall. Ex-situ data detected by the MODIS AQUA-L3SMI satellite a month or three months vary widely. Water has good heat-specific properties, meaning that the increase or decrease in heat occurs slowly. The sea surface can absorb a large amount of solar energy that enters it. When it evaporates, the sea surface becomes hot. When heated, warm water remains on the surface while cold water sinks or is at the bottom. The energy that reaches the earth's surface varies according to seasons, latitude, and topography (Ingmanson and Wallace, 1973).

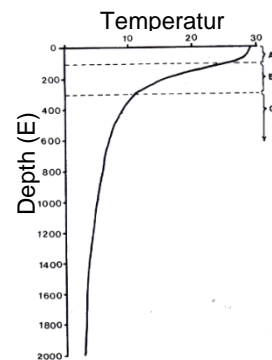


Fig 17. The general vertical distribution of temperature in Indonesia Waters (Nontji, 1987).

The temperature of seawater in the surface layer is highly dependent on the amount of heat received from sunlight. According to Hela and Laevastu (1970), changes in sea surface temperature, apart from being caused by the amount of heat received from the sun, are also influenced by natural conditions and the surrounding environment in the waters. The influence of currents, cloud conditions, rising water masses, and melting of polar ice also affects the temperature at sea level.

Sverdrup *et al.*, (1942) said that, processes such as absorption of radiation from the sun, the flow of heat from the earth through the seabed, changes in the form of kinetic energy into heat energy, the flow of heat from the atmosphere through the air to the sea and condensation of water vapor accompanied by the release of heat. The heat that occurs in the ocean will increase the temperature of the seawater. Furthermore, the processes of back radiation from the sea surface, heat flow (convection) to the atmosphere, and evaporation can reduce the temperature of seawater in the surface layer of the waters.

Conclusion

Based on the results of the analysis of the SST study and the containing water of chlorophyll-a using MODIS AQUA-L3SMI imagery, the analysis shows that the SST value and chlorophyll-a containing water in 2019 in the rainy and dry seasons, high and low, have varied values, so the influence of the season can determine the direction of the distribution pattern. SST and chlorophyll-a containing water, both tidal factors and weather conditions such as rain and drought. The effect of tides on SST distribution patterns and chlorophyll-a containing water in Sibolga Waters causes SST values and chlorophyll-a containing water at high tide to be higher than at low tide. MODIS AQUA-L3SMI imagery can be used to map the distribution pattern of SST and chlorophyll-a containing water in the Sibolga Waters area.

BIBLIOGRAPHY

Book

- Arinardi. 1995. Distribution of Seston, Chlorophyll-a, and Bacteria in Jakarta Bay. Jakarta Bay Oseanology Atlas. Chapter VI: 101-9. Jakarta.
- Butler, M. J. A., Mouchot, M. C., Barale, V., Le Blanca, C. 1988. The Application of Remote Sensing Technology to Marien Fisheries. An Introduction Manual. FAO Fisheries Technical Paper. 295 p.
- Ingmanson, D.E., Wallace, W. J. 1973. Oceanology: An Introduction. California: Wadsworth. Belmont. 325 p.
- Kushardono, B. 2003. Remote Sensing Technology in Coastal and Ocean Area Management. In: Trisakti B, Hasyim B, Dewanti R, Hartuti M, Winarso G, editor. Jakarta: Center for Development of Utilization and Remote Sensing Technology of the National Aeronautics and Space Administration. 12-18 p.
- Laevastu, T and Hayes, M. L. 1970. *Fisheries Oceanography and Ecology*. Fishing News Books Ltd. England. 199 p.
- Laevastu, T and Hayes, M. L. 1981. *Fisheries Oceanography and Ecology*. Fishing News Books Ltd. England. 199 p.
- LIPI. 2007. Coral Reef Information and Training Center Coral Reef Rehabilitation and Management Program. Indonesian Institute of Sciences CRTICCOREMAP II. Jakarta. 47 p.
- Muhsoni, F. F. 2015. Remote Sensing. UTM Press. Trunojoyo University. Madura.
- Nontji, A. 1987. Nusantara Sea. First print. Djambatan Publisher. Jakarta. 360 p.
- Sverdrup, H. V., Johnson, M. W., Fleming, R. H. 1942. *The Oceans: Their Physics, Chemistry, and General Biology*. Englewood: Prentice Hall Inc.

Proceeding

- Aboet, A. 1985. Satellite Remote Sensing an Alternative for Oceanographic Research.

Proceedings of the Workshop on Utilization of Environmental and Weather Satellite Data, 18-19th September 1985 in Jakarta. 214-230 p.

- Hasyim, B. 1999. Analysis of Sea Surface Temperature Distribution and Its Relation to Fishing Locations. Proceedings of the Sensory Data Validation Seminar for the Fisheries Sector. Jakarta 14th April 1999. Agency for the Assessment and Application of Technology (BPPT). Jakarta. ISBN: 979-956760-1-6: III-2-III-46.

Journal

- Arinardi, O., Trimaningsih, H., Sudirdjo, Sugestiningsih., Riyono, S. H. 1997. Range of Predominant Plankton Abundance and Composition in Eastern Indonesian Waters. Oceanology Research and Development Center. Indonesian Institute of Sciences. Indonesia Journal of Fisheries Research Vol. 11 No. 6 of 2005. Jakarta. 128 p.
- Gabric, A. J and Parslow, J. 1989. *Effect of Physical Factors on the Vertical Distribution of Phytoplankton in Eutrophic Coastal Waters*. Australian Journal Marine Freshwater. Res., 189,40,559-569.
- Nababan, B. 2016. Variability of Sea Surface Temperature and Chlorophyll-a Concentration in Jakarta Bay and Surrounding Waters. Journal of Tropical Marine Science and Technology. (1): 385-402.
- Parson, R. T., Takeshi, M and Hargrave, B. 1984. *Biological Oceanography Process*. 3rd edition. Pergamon Press. Oxford. England, 330. International Journal of Remote Sensing and Earth Sciences Vol. 2 September 2005. 94 p.
- Setiapermana, D., Santoso and Riyono, S. H. 1992. Chlorophyll-a Containing water in Relation to Physical Structure in East Indian Ocean. Research and Development Center for Oceanology-LIPI. Jakarta.

Thesis

- Sinaga, M. P. 2009. Analysis of Trawler Catches about Containing Water Chlorophyll-a and Sea Surface Temperature in Tapanuli Tengah Waters.

Website

- Maccherone, B. 2005. About MODIS. <http://modis.gsfc.nasa.gov/> [accessed date 12nd September 2019].
- NOAA. 2008. National Oceanic and Atmospheric Administration Satellite. <http://www.noaaa.gov/satellites.html>. Accessed date 17th September 2019.